Original paper

https://doi.org/10.22201/igeof.00167169p.2021.60.4.2119

Wavelet-based Characterization of Seismicity and Geomagnetic Disturbances in the South Sandwich Microplate Area

P. Larocca[1]* M. A. Arecco[1,2] y M. Mora[1]

Recived: November 24, 2020; accepted: Jun 21, 2021; published online: October 1, 2021.

Resumen

En este trabajo se analizan perturbaciones geomagnéticas relacionadas con eventos sísmicos localizados en el margen transcurrente norte de la micro Placa de Sandwich del Sur y la placa Sudamericana, con epicentro a distancias menores de 350 km del observatorio geomagnético King Eduard Point en el archipiélago de las islas Georgias del Sur.

Se estudian registros del campo geomagnético medido en tres observatorios de la red INTERMAGNET próximos a la zona de estudio en un lapso de 1 año. Es posible detectar variaciones anómalas en los registros geomagnéticos en lapsos de aproximadamente 3 horas antes de la manifestación de eventos sísmicos de magnitud superior a 4,4 Mw.

A partir del análisis de las diferencias entre las componentes horizontales del campo de los observatorios King Eduard Point y Orcadas y el espectro de frecuencias de las observaciones de campo geomagnético, a partir del método de wavelet es posible observar oscilaciones de varios nT previas al evento, además de picos magnéticos de amplitud y duración variable.

Cabe destacar que en el periodo de estudio no se registraron tormentas geomagnéticas intensas o superintensas por encontrarse en fase de baja actividad solar (mínimo de ciclo solar 24).

La observación de estos posibles premonitores magnéticos sugiere que hay un tiempo de preparación crítico en una región de fallas geológicas relacionado con la tensión generada en las rocas previo a la liberación de la energía acumulada en la zona del hipocentro, en el interior de la litosfera, que podría anticipar el movimiento mecánico a partir de registros geomagnéticos anómalos.

Palabras clave: variaciones geomagnéticas, sismos, índices de actividad geomagnética.

*Autor de correspondencia: *plarocc@fi.uba.ar*

[1] *Universidad de Buenos Aires, Facultad de Ingeniería, Instituto de Geodesia y Geofísica Aplicadas, Buenos Aires, Argentina.*

[2] *Universidad de la Defensa Nacional, Instituto Universitario Naval, Escuela de Ciencias del Mar, Buenos Aires, Argentina.*

Abstract

This paper analyzes geomagnetic disturbances associated with seismic events in the northern transcurrent margin of the South Sandwich microplate and South American plate, with their epicenter at distances within 350 km from King Edward Point geomagnetic observatory on the archipelago of the Georgias del Sur islands.

Geomagnetic field records measured over a one-year period in three observatories of the INTERMAGNET network near the area under study are examined. Anomalous variations in geomagnetic records can be detected within approximately 3 hours before the manifestation of seismic events with a magnitude above 4.4 Mw.

Based on the analysis of the differences in horizontal field components among the observatories and the frequency spectrum of the geomagnetic field observations using the wavelet method, oscillations of several nT can be observed before an event, in addition to magnetic peaks with variable amplitude and duration.

It is worth noting that, during the period of study, no severe geomagnetic storms were recorded as this was a phase of low solar activity (solar cycle 24 minimum).

The observation of these potential magnetic precursors suggests that there is a critical preparatory period in a region with geological faults related to the stress generated in the rocks before the built-up energy is released in the hypocenter area, within the lithosphere, which may possibly predict the mechanical motion based on anomalous geomagnetic records.

Key words: geomagnetic variations, earthquakes, geomagnetic activity indices.

Introduction

One of the most elusive objectives for seismology is being able to predict an earthquake in the short term. There are numerous studies reporting relationships between earthquakes and physical phenomena, such as significant mechanical effects in the focal area of an earthquake, whether rock changes or deformation; changes in rock properties and stress-deformation state; changes in the chemical composition and/or temperature of the groundwater; electrophysical properties of the medium; increased emanations of natural radon and excitation of seismic signals: all of this affects the regimes of geophysical fields (Hayakawa *et al.* 2010; Takeuchi *et al.* 2012, Varotsos *et al.*, 2013; Spivak and Riabova, 2019).

The geomagnetic field is no exception. It was repeatedly observed that geomagnetic field disturbances occurred during the preparation stage of an earthquake (Kushwah *et al.*, 2009; Ruiz *et al.*, 2011; Takla *et al.*, 2018).

The geomagnetic field that is measured on the earth's surface is the vector sum of various constituent fields, each of which has a different origin and varies differently in time and space. It is mainly made up of two constituents: a global one with great amplitude, whose source is within the earth, and the other one, with a much lesser amplitude, created by more superficial sources. Onlapping them is the outer field caused by electric currents circulating in the ionosphere and the magnetosphere which, when varying in time, generate induced fields. (Mandea and Purucker, 2005, Tackla *et al.*, 2018).

Over 90 percent of the measured field is generated in the outer core of the earth. This part of the geomagnetic field slowly varies in time and can be described by means of mathematical models, such

as the International Geomagnetic Reference Field (IGRF) and the World Magnetic Model (WMM) (Alken *et al.*, 2021, Rother *et al.*, 2021).The intensity of the magnetic signal from rocks is usually below 1 percent of the intensity of the earth's main magnetic field. However, with a geomagnetic field model (for example, the IGRF), these small signals may be recovered from the data measured (Skordas and Sarlis, 2014). Geomagnetic studies can contribute to providing information on the subsoil and the process involving an earthquake.

There are a lot of studies on the mechanisms (Ryu *et al.* 2014) that cause the ionospheric disturbances coupled to seismic activities. Furthermore, recent statistical studies using ground and satellite data have provided convincing correlations between the seismic activities and the ionospheric disturbances preceding earthquakes [Fujiwara *et al.*, 2004; Liu *et al.*, 2006, Larocca *et al.*, 2019].

The analysis of indices of solar and geomagnetic activity serves to account for how rapid variations of geomagnetic activity influence data processing. Dst, Ap and F10.7 cm indices are usually used to monitor this phenomenon (Tsurutani *et al.*, 1997, 1999). The intensity of the equatorial magnetic field, measured by the *Dst* index, is directly related to the total kinetic energy of the ring current particles (Rostoker *et al.*, 1997), thus, the *Dst* index is also often used to determine whether or not a storm occurred, to define the duration of a storm, and to distinguish between quiet and disturbed geomagnetic conditions. *Ap* index characterizes the intensity of geomagnetic activity at planetary scale from the measurement of the horizontal component of the magnetic field observed in 13 stations, of which 11 correspond to the northern hemisphere and two to the south and the solar index F10.7cm measures the radio emissions *F10.7*cm that originate in the upper atmosphere (Perrone & De Franceschi, 1998).

The subduction zone of the South American plate beneath the South Sandwich plate, located in the South Atlantic, is one of the areas with highest seismic activity in the planet —within a year, over 300 seismic events of Mw > 4.1 may occur. This small plate is bounded to the north and east by the South American plate; to the south, by the Antarctic plate; and to the west, by the Scotia plate. The subduction zone shows an active volcanic and tectonically simple intra-oceanic arc. The active arc is largely built on the oceanic crust of the small South Sandwich plate, which was formed approximately 10 Ma ago in the spreading center of the East Scotia ridge (Leat *et al.*, 2003). The arc is being formed in response to an inclined subduction of the South American plate beneath the South Sandwich plate at a velocity of 67–79 km / Ma (Thomas *et al.*, 2003); within a year it accounts for a relative displacement of 7 to 8 cm.

This paper sets out to examine the occurrence of any changes in the earth's magnetic field associated with seismic events of the small South Sandwich plate, in a one-year period from May 17, 2018 to the same date in 2019. To this end, magnetic data records of three observatories closest to the study area were studied, namely King Edward Point (KEP), located in the vicinity, Port Stanley (PST) on the Malvinas islands, and Orcadas (ORC) on the Orcadas del Sur islands, located farther away, in the cited period based on filter processing and wavelet analysis of their differences.

Data and Methodology

This paper used the value of the International Geomagnetic Reference Field available at https://www.ngdc.noaa.gov/geomag/data.shtml as a reference value for the three magnetic observatories, which was then subtracted from their daily observations for the one-year period between May 17, 2018

and May 17, 2019. Data were acquired per minute from observatories King Edward Point (KEP) (54.3° S; 36.5° W), located in the vicinity of the transcurrent margin, Port Stanley (PST) (51.7° S; 57.8° W), and Orcadas (ORC) (60.7° S; 44.7° W). These data were obtained from the International Real-time Magnetic Observatory Network (INTERMAGNET) with a 1-minute resolution, available at https://intermagnet.github.io.

Nearly 300 seismic events of Mw > 4.4 and their respective depths, as extracted from the United States Geological Survey (USGS, https://earthquake.usgs.gov/earthquakes/), were analyzed (Figure 1).

In addition, in order to take into account the rapid variations of the geomagnetic field, this study included information from geomagnetic indices *Dst, Ap* and the solar index F10.7cm. Dst —monitoring the variations of the horizontal component of the earth's magnetic field due to an increase in the ring current derived from a network of geomagnetic observatories symmetrically located in the equatorial area, and measured in nT. The value of the *Dst* index is statistically zero on days considered quiet. *Dst* index is reported by Kyoto University in hourly values. During a geomagnetic storm, its value falls to a minimum value and then recovers to zero. According to the minimum value reached, the onset of an intense storm is considered if *Dst*> -100 nT (Sugiura and Chapman, 1960; Sugiura, 1964), which does not occur in our study period. *Ap* index is reported daily, nevertheless its sampling rate is supposed to be three hourly. Values of *Ap* > 40 nT provide a maximum disturbance measure useful to identify major geomagnetic storms (Perrone and De Franceschi, 1998) but in these periods of time, they are lowest; and *F10.7 cm* solar index is an excellent indicator of the solar activity originating high in the chromosphere and in the corona of the solar atmosphere, and it is reported in "solar flux units" (sfu); as obtained from the Geomagnetic Data Service of Kyoto (http://wdc.kugi.kyoto-u.ac.jp/wdc/Sec3.html). On the other hand, the value of the radio flux index was always below 70 sfu.

The methodology used involved studying intervals with a length from 7 to 10 days, which included seismic events, throughout the year. Because the closest Geomagnetic observatory to the study area is KEP Observatory, it was decided to focus the study on the analysis of the data recorded there.

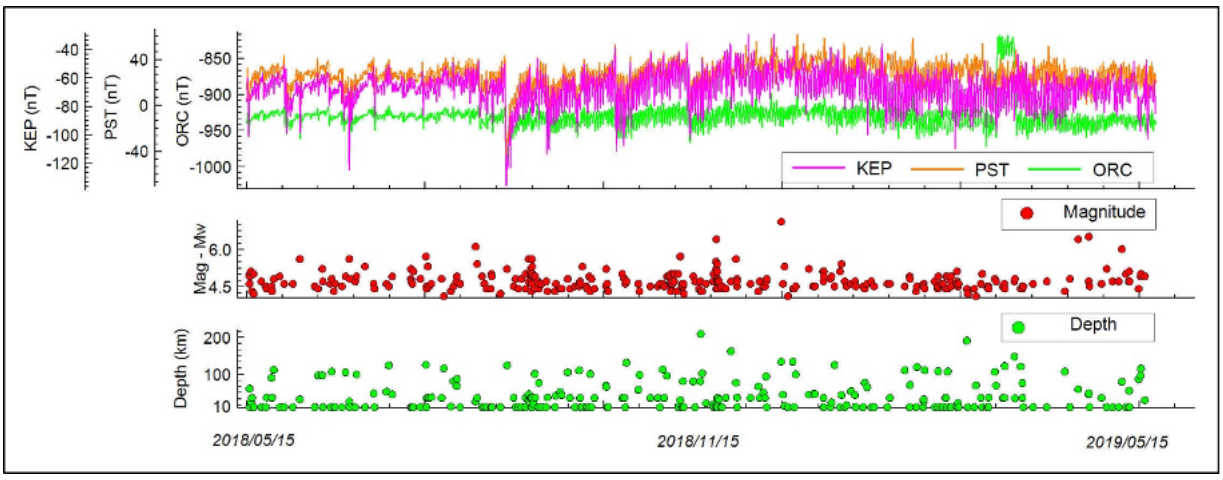

Figure 1. Daily variations of the H component of the earth's magnetic field in PST, KEP and ORC observatories. Magnitudes of earthquakes and their depths during the year of study.

The technique to identify potential anomalous variations of the earth's magnetic field implied examining the wavelet power spectra of magnetic data from KEP Magnetic Observatory, separately analyzing the horizontal and vertical components of the magnetic field measured, and subsequently analyzing the horizontal component with the application of a low pass filter to attenuate the diurnal anomaly (Grinsted *et al.*, 2004) and to be to identify anomalous frequencies around the earthquake detection time.

In addition, in such intervals, for the purposes of isolating the magnetic field caused by the local geomagnetic variation due to solar variability, the field differences (Δ) between KEP and ORC observatories (Δ KEP-ORC) were calculated, the value of the reference magnetic field corresponding to the time and location of each observatory was subtracted. This procedure was used to accentuate the effects of seismic activity given KEP's proximity to the South Sandwich plate. Afterwards, wavelets (wt) were applied with Morlet exponential decay to the time series obtained from the difference of the data recorded (only the horizontal component of the geomagnetic field is analyzed as it is most susceptible to its rapid variations).

Results

Seven representative seismic events were chosen to describe the results obtained (Table 1). These events were selected due to their closeness to King Edward Point observatory (less than 350 km).

Table 1.Selected seismic events close to King Edward Point geomagnetic observatory.

No.	Date	Time	Lat. (°)	Long. (°)	Depth (km)	Mag	Type of Mag.	Place
*1	5/24/2018	12:47	-54.9892	-32.118	10	4.5	Mb	294km ESE of Grytviken
*2	7/05/2018	19:23	-55.096	-30.9409	10	4.4	Mb	240km ESE of Grytviken
*3	9/21/2018	19:07	-55.0491	-33.4245	10	4.5	Mb	216km ESE of Grytviken
*4	9/26/2018	05:28	-55.3485	-31.3375	10	4.5	Mb	298km WNW of Visokoi Island
*5	9/26/2018	14:31	-55.0642	-31.3753	10	4.4	Mb	298km WNW of Visokoi Island
*6	10/11/2018	09:49	-55.1947	-30.9411	10	4.6	Mb	287km NW of Visokoi Island
*7	4/05/2019	16:14	-55.9206	-27.856	58.6	6.4	Mb	95km NW of Visokoi Island

The events selected occurred during periods characterized by the absence of significant magnetic activity manifestations, resulting from the analysis of the geomagnetic indices *Dst, Ap* and the solar index *F10.7cm* as qualitative indicators of the activity, as shown on Figure 2. During the solar minimum the large-scale dynamics of the interplanetary medium is dominated by the stream interaction regions, which they produce most of the small and moderate geomagnetic storms during this period. The space weather events during the solar minimum, are mainly associated with stream interaction regions. Then the geomagnetic activity is not produced by solar flares o coronal mass ejections, but by interaction regions.

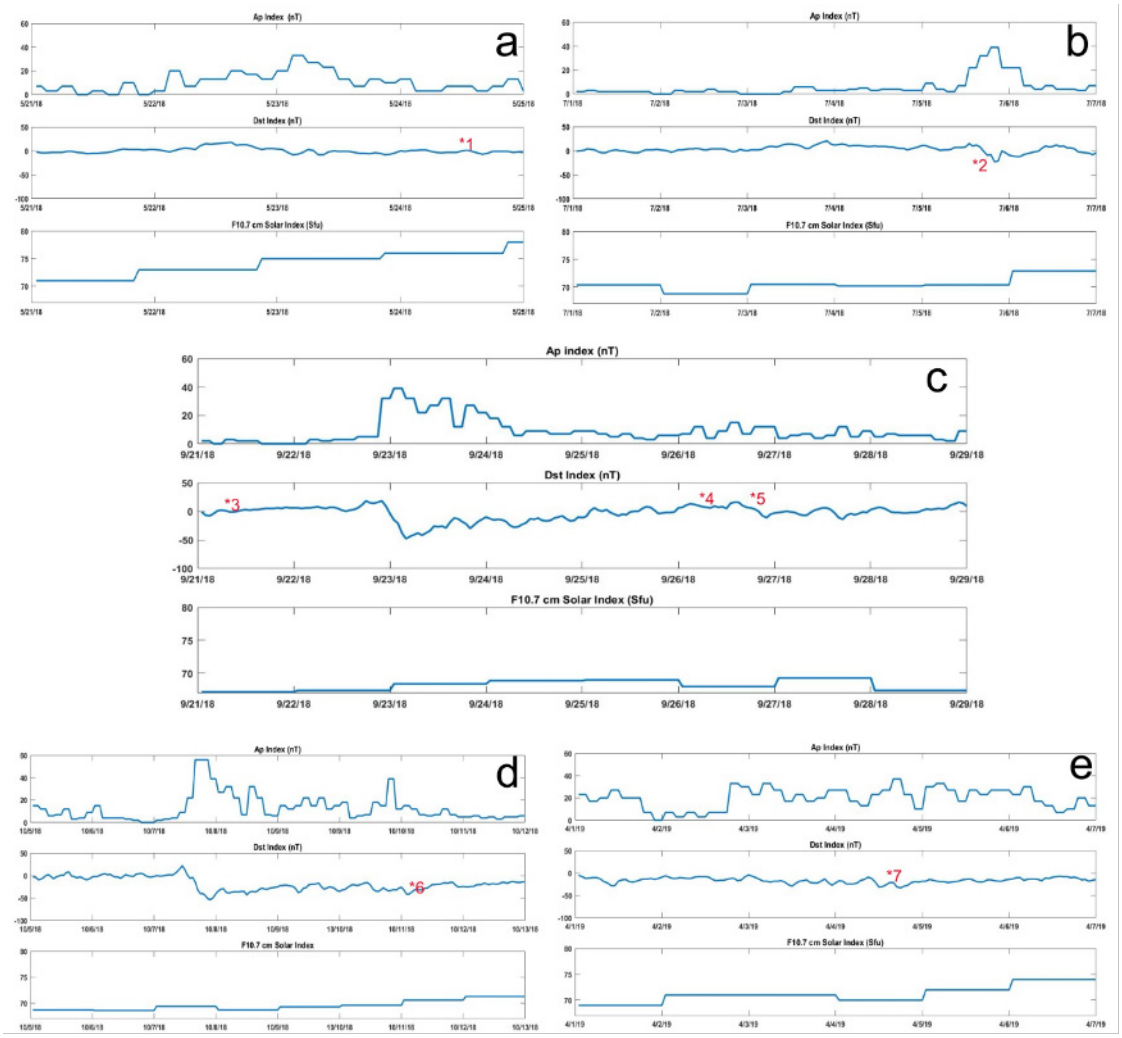

Figure 2. Solar indices *Ap* (nT), *Dst* (nT) and *F10.7* cm (SFU=10^{-22} Wm^{-2} Hz^{-1}) corresponding to periods 21-26 May, 2018; 1-7 July, 2018; 20-27 September, 2018; 5-13 October, 2018; and 1-7 April, 2019.These indices account for a low solar activity period.

Storm type according to Loewe & Prolss (1997) can be classified: a weak storm if it has –30 nT > *Dst* > –50 nT, a moderate storm if it has –50 nT > *Dst* > –100 nT, a strong storm if it has –100 nT > *Dst* > –200 nT, a severe storm : –200 nT > *Dst* > –350 nT, and a great storm with *Dst* < -350 nT. Then, in the selected periods, only two weak storms were observed on 9/22/18 and 10/8/18 with *Dst* ~-48 nT. The study shows that the small geomagnetic variations, presumably associated with seismic events, there were not in fact driven by solar wind stream interactions hitting the Earth's environment because they do not temporarily match those chosen for observation.

For the seven events selected, the magnetic field determined in KEP observatory was plotted, including both its horizontal and vertical components, showing anomalous variations in both components before a seismic event, although with better resolution in the horizontal component. In order to subtract the contribution of the diurnal solar variation and some weak events associated with space weather phenomena, the difference between the horizontal components from KEP and ORC observatories was calculated, and it was subsequently applied a low-pass filter (filtered signal). For

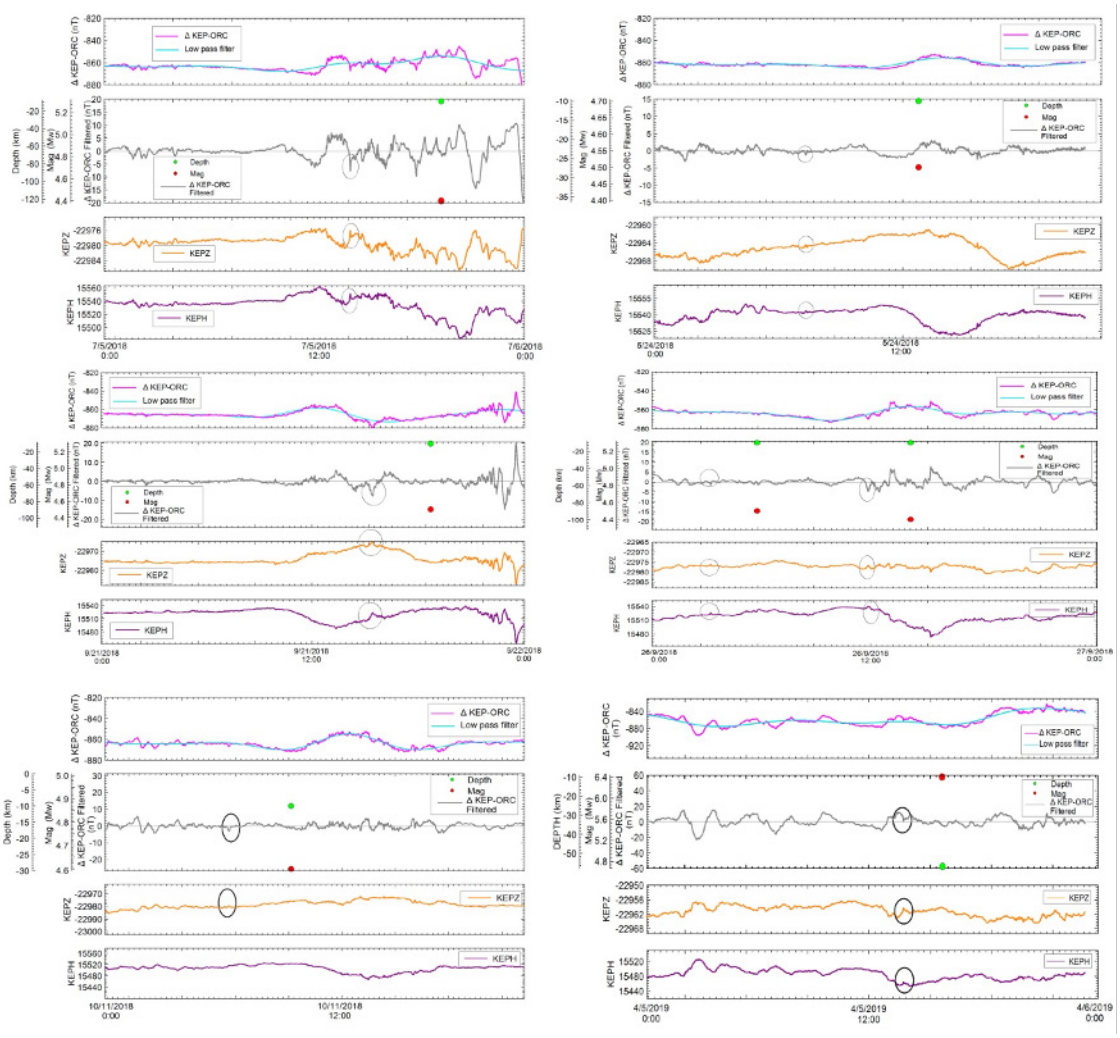

Figure 3. Magnetic data of 24 May, 2018; 5 July, 2018; 21 and 26 September, 2018; 11 October, 2018; and 5 April, 2019. Difference between magnetic data from KEP and ORC observatories.

the purposes of finding small field variations, the differences between Δ KEP-ORC and the filtered signal, were calculated (Figure 3). In all the seismic events, peaks were seen both in the H and Z components, as well as in the filtered variation, as shown on Table 2.

Table 2. Intensity of the peaks observed in figure 3 on the difference of the magnetic data recorded in the KEP and ORC observatories and their anticipation to seismic events.

No.	Date	Magnitude	Peak intensity (nT)	Anticipation (hours)
*1	05/24/2018	4.5	1.56	2h 47m
*2	07/05/2018	4.4	4.4	5h 10m
*3	09/21/2018	4.5	7.58	3h 30m
*4	09/26/2018	4.5	1.49	3h 00m
*5	09/26/2018	4.4	3	2h 30m
*7	04/05/2019	6.4	3.1	2h 07m

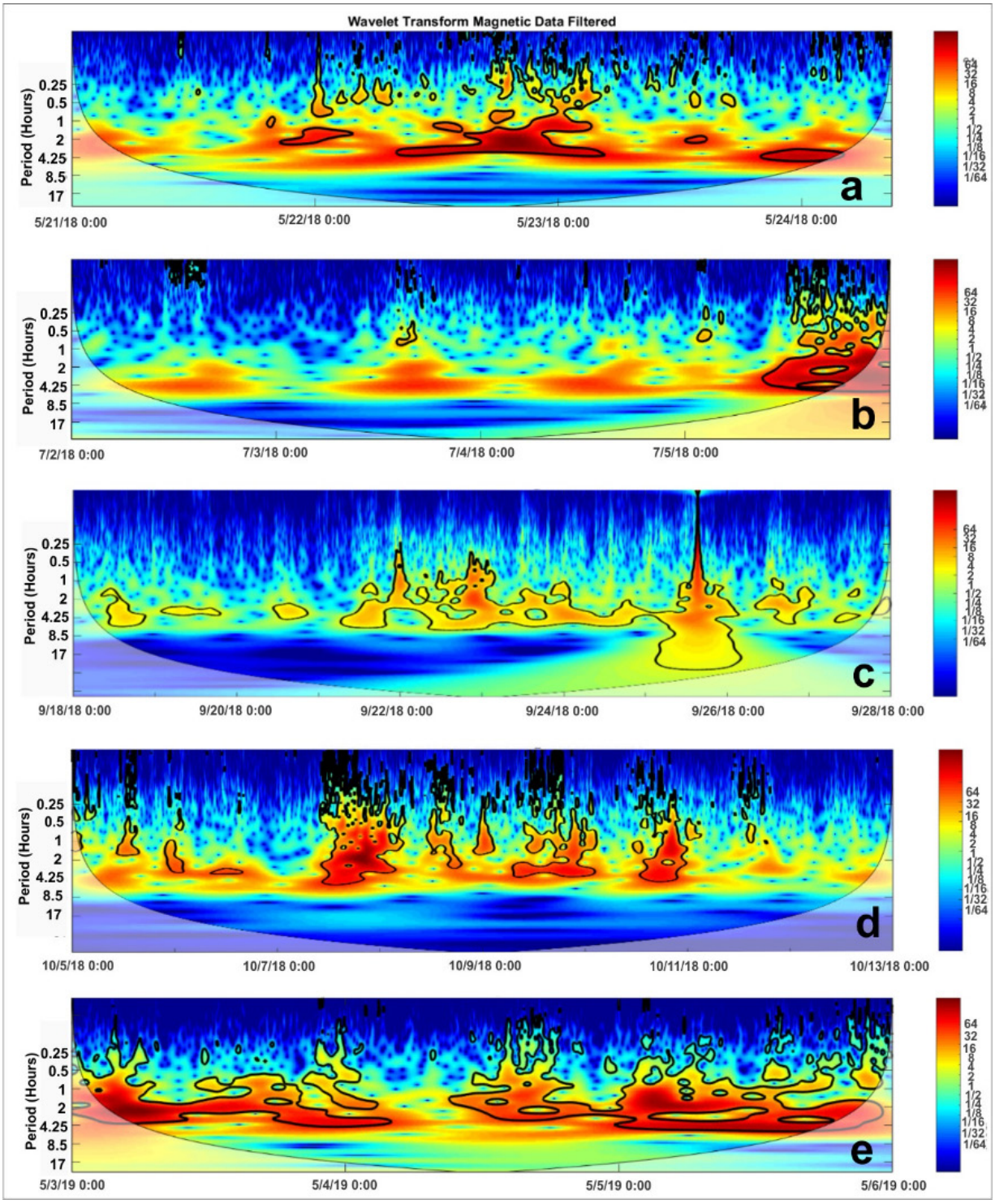

Figure 4. Continuous wavelet transform of the periods from 21 to 24 May, 2018; from 2 to 6 July, 2018; from 18 to 28 September, 2018; from 5 to 12 October, 2018; and from 3 to 6 April 2019 for ΔKEP-ORC The data shown corresponds to the difference between the horizontal components of the magnetic records of the KEP and ORC observatories, where the corresponding local IGRF contribution had already been discounted. These data were called: Filtered data in the figure. The thick black contour shows a 5% significance level against the red noise background, and the cone of influence (COI) where the edge effects may distort the image is blurred.

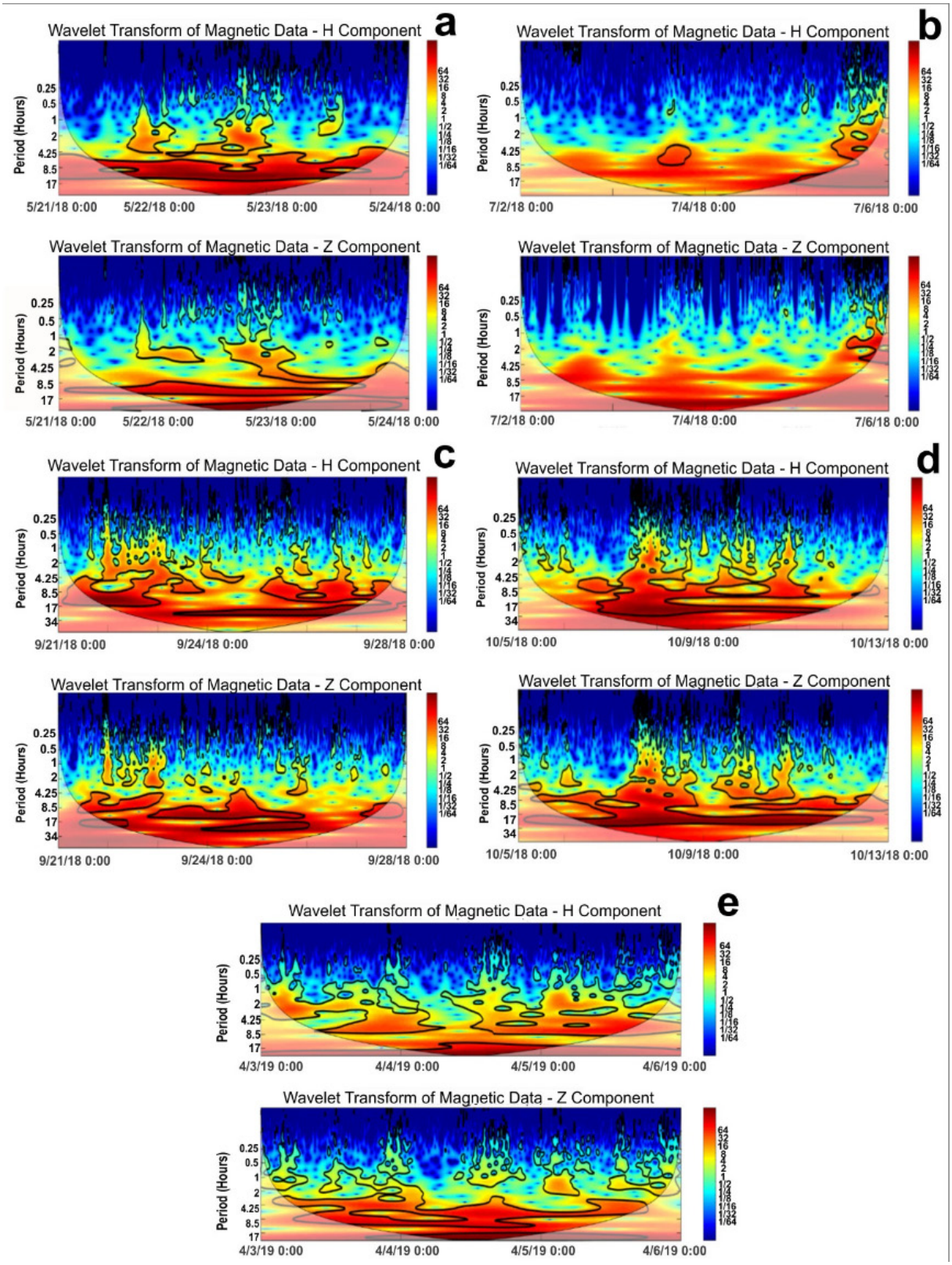

Figure 5. H and Z from 18 to 28 Septembercorresponding to the periods from 21 to 24, May 2018; from 2 to 6 July, 2018; from 18 to 28 September, 2018; from 5 to 12 October, 2018; and from 3 to 6 April, 2019.

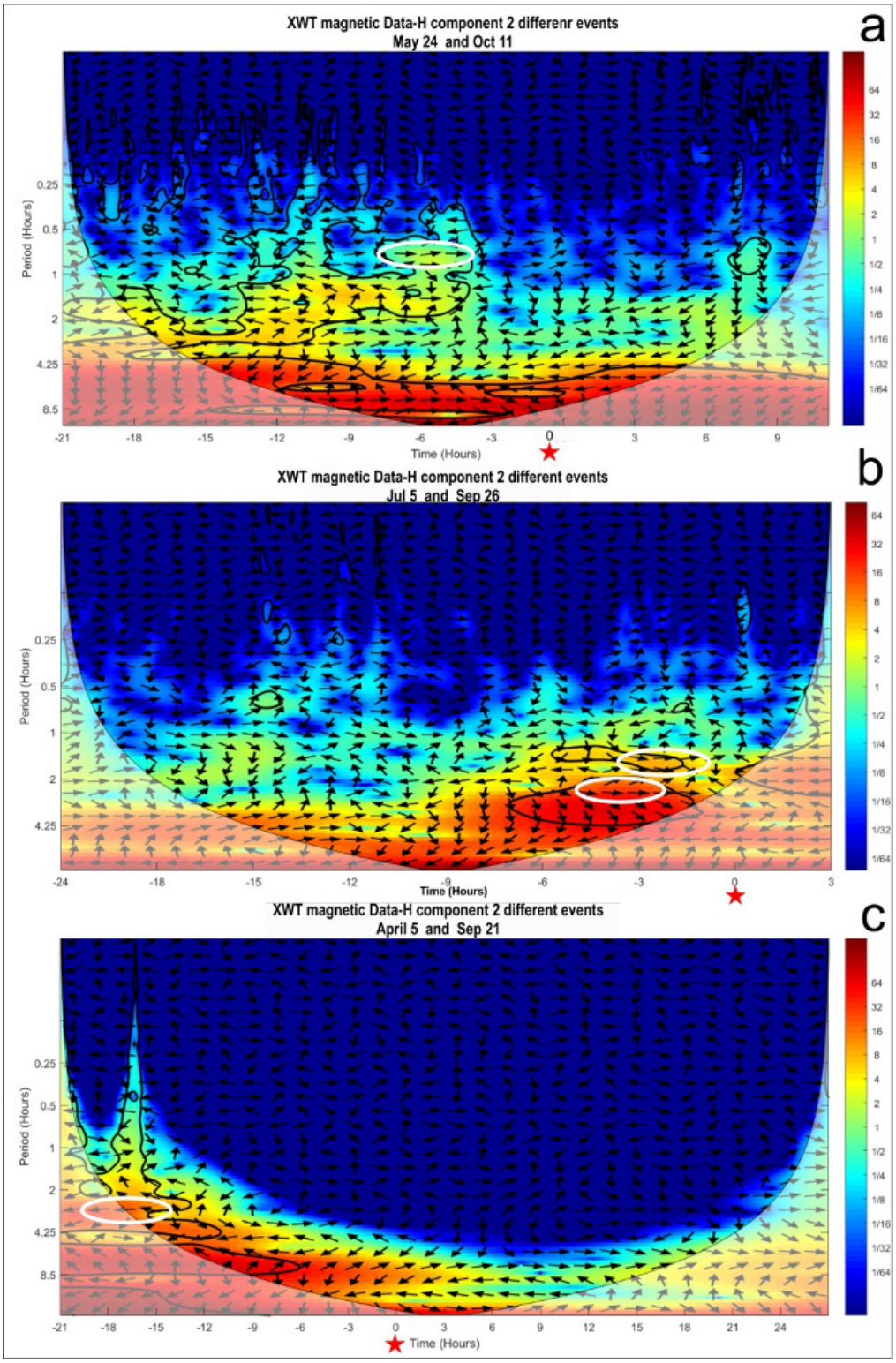

Figure 6. Geomagnetic field XWT from KEP observatory for the following events: a) 24 May and 11 October, 2018; b) 5 July and 26 September, 2018; and c) 21 September, 2018 and 5 April, 2019. Seismic event coincidence instant (red star) and coherent phase (white oval). The arrows show the relative phase (with the phase pointing to the right and the anti-phase pointing to the left).

In addition, the continuous wavelet transform (WT) was applied both to ΔKEP-ORC (Figure 4) and to each H and Z component of the magnetic field observed in KEP (Figure 5). The Morlet wavelet (with $\omega_0 = 6$) was used, as it provides a good balance between the time and frequency location. Figures 4 and 5 show the periodic oscillation of these magnetic data from 21 to 24 May, 2018; from 2 to 6 July, 2018; from 18 to 28 September, 2018; from 5 to 12 October, 2018; and from 3 to 6 April, 2019.

We examined two time series whose interval had the earthquake occurrence moment as a common instant. For the purposes of correlating periodicities between both series, we inspected these series together so as to find common frequencies. Based on their WTs, we constructed the Cross Wavelet Transform (XWT), which exposes their common power and relative phase in the time-frequency space. We used the corresponding software at http://noc.ac.uk/using-science/crosswavelet-wavelet-coherence. Figure 6 shows the result.

We applied a measure of the coherence between both WTs, referred to as wavelet transform coherence (WTC), so as to find significant coherence. If both series are physically related, we should expect a consistent or slowly varying phase. Monte Carlo methods are used to assess the statistical significance against red noise backgrounds.

There are clearly common characteristics in the wavelet power of the paired series, showing on Figure 6 a) and b) very good correlation in the interval between 6 and 4 hours before the occurrence of an earthquake corresponding to a period between 2 and 0.5 hours. For Figure 6 c), the correlation is inverse and it occurs more than 15 hours earlier.

Conclusions

Potential magnetic precursors could be identified for events with a magnitude above 4.4 Mw.

In all the events, peaks between 1.5 and 4.4 nT were observed in the filtered variation around 3 hours before a seismic event, and a 7.58 nT peak corresponding to the earthquake closest to KEP observatory outstands. Their association with solar storms is ruled out as this is a solar minimum period.

The filtering operation to yield the filtered variation was effective, as the wavelet transform studies do not show periods for 24 hs, 12 hs or 6 hs.

When observing the wavelet transform both in the horizontal H and vertical Z components, high coherence was found around the corresponding 2 to 0.25 hour band, which increases over a period near the occurrence of a seismic event, but, as no filters were applied in this case, the diurnal and semi-diurnal components are those with highest energy.

The study of time correlation among seismic events, such as those on 24 May and 11 October, 2018; 5 July and 26 September, 2018; and 21 September, 2018 and 5 April, 2019, using an independent method based on the Cross Wavelet Transform (XWT) (Grinsted *et al.*, 2004), showed that, in a period from 2 to 3 hours before an earthquake, there is high coherence between both analyses, which may be characterizing an alteration in the magnetic field due to seismic activity. This period increases to over 15 hours when the comparison involves a deeper and more intense earthquake, but farther away from the location where the magnetic field is recorded.

It would be inferred that there is a connection between geomagnetic variations and seismic events, nevertheless some signals show similar signatures as those highlighted and not associated to earthquakes.

Further evidence is needed for a better assessment of potential geomagnetic phenomena associated with earthquakes, which is why continuous monitoring is intended over a longer period, including more significant events making it probable to find possible correlations with seismic activity.

Acknowledgements

We thank the referees for their valuable comments.

This work has been supported by the research projects of Science and Technology of the University of Buenos Aires, Argentina, No. 200201601000088BA (UBACYT) and Strategic Research of the University of National Defense No. 279/2018 (UNDEFI), Argentina.

Wavelet software was provided by C. Torrence and G. Compo, and is available at URL: http://atoc.colorado.edu/research/wavelets/.

References

Alken, P., Thébault, E., Beggan, C.D. et al., 2021. International Geomagnetic Reference Field: the thirteenth generation. *Earth Planets Space*, 73, 49. doi: 10.1186/s40623-020-01288.

Fujiwara, H., Kamogawa, M., Ikeda, M., Liu, J. Y. , H. Sakata, H., Chen, Y. I., Ofuruton, H., Muramatsu, S., Chuo, Y. J. and Ohtsuki, Y. H., 2004. Atmospheric anomalies observed during earthquake occurrences, *Geophys.* Res. Lett., 31, L17110. doi:10.1029/2004GL019865.

Grinsted, A., Moore J. C., and Jevrejeva S., 2004. Application of the cross wavelet transform and wavelet coherence to geophysical time series. *Nonlin.* Process. *Geophys.*, 11, 561-566.

Hayakawa, M., Kasahara, Y., Nakamura, T., Muto, F., Horie, T., Maekawa, S., Hobara, Y., Rozhnoi, A. A., Solovieva, M., and Molchanov, O. A. (2010), A statistical study on the correlation between lower ionospheric perturbations as seen by subionospheric VLF/LF propagation and earthquakes, *J. Geophys. Res.*, 115, A09305, doi:10.1029/2009JA015143.

INTERMAGNET International Real-time Magnetic Observatory, https://intermagnet.github.io, last modified date: 2020-02-02.

Kushwah V, Singh V, and Singh B., 2009, Ultra-low frequency (ULF) amplitude observed at Agra (India) and their association with regional earthquakes. *Phys.Chem Earth.* 34, 367–272.

Larocca, P., Fiore, M., Oreiro F., Vilariño, I. and Arecco, M.A., 2019. Estudio de parámetros geo-magnéticos y su posible influencia sobre anomalías sismo-ionosféricas. In Proceedings of the Sixth Biennial Meeting of Latinmag, Fernando Poblete, C. I. Caballero M, (Eds), *Latinmag Letters*, 9, Special Issue, A18-P, 1-6.

Leat, P.T., Smellie, J.L., Millar, I.L. and Larter, R.D., 2003. Magmatism in the South Sandwich arc. In: Larter, R.D., Leat, P.T. (Eds.), *Intra-Oceanic Subduction Systems: Tectonic and Magmatic Processes.* Geological Society, London Special Publications, 219, 285–313.

Liu, J. Y., Y. I. Chen, Y. I., Chuo, Y. J. and Chen C. S., 2006. A statistical investigation of preearthquake ionospheric anomaly, *J. Geophys. Res.*, 111, A05304, doi:10.1029/2005JA011333.

Loewe, C. A., and Prölss, G. W., 1997. Classification and mean behavior of magnetic storms, *J. Geophys. Res.*, 102 (A7), 14209– 14213, doi:10.1029/96JA04020.

Mandea, M. and Purucker, M., 2005. Observing, Modeling and Interpreting Magnetic Fields of the Solid Earth. *Surv Geophys* 26, 415–459. doi: 10.1007/s10712-005-3857-x

Perrone L., and De Franceschi G., 1998. Solar, ionospheric and geomagnetic indices, Ann. Geofis., 41 (5-6), 843-855.

Rostoker, G, Friedrich, E. and Dobbs, M., 1997. Physics of magnetic storms. *Magnetic storms*, 98, 149-160.

Rother M., Korte M., Morschhauser A. , Vervelidou F., Matzka J. and Stolle C., 2021. The Magnum core field model as a parent for IGRF-13, and the recent evolution of the South Atlantic Anomaly. *Earth, Planets and Space*, 50-73. https://doi.org/10.1186/s40623-020-01277-0.

Ruiz, F., Sánchez, M., Martínez. P., Giménez, M., Leiva, F., Álvarez, O. and Introcaso, A., 2011. La estación magnética Zonda: estudio de perturbaciones magnéticas relacionadas con terremotos. San Juan, Argentina. *Latinmag Letters*, 1, Special Issue, A16, 1-7.

Ryu, K., Parrot, M., Kim, S. G., Jeong, K. S., Chae, J. S., Pulinets, S. and Oyama K. I.. 2014. Suspected seismo-ionospheric coupling observed by satellite measurements and GPS TEC related to the M7.9 Wenchuan earthquake of 12 May 2008, *J. Geophys. Res. Space Physics*, 119, doi:10.1002/2014JA020613.

Skordas E. S. and Sarlis N. V., 2014. On the anomalous changes of seismicity and geomagnetic field prior to the 2011 Mw 9.0 Tohoku earthquake. *Journal of Asian Earth Sciences*. Elsevier 80, 161-164Ltd. doi.org/10.1016/j.jseaes.2013.11.008.

Spivak, A. A., and Riabova, S. A., 2019. Geomagnetic Variations during strong earthquakes. *Physics of the Earth*, 6, 3-12. Doi: 550.385.37:550.388.

Sugiura, M., 1964. Hourly values of equatorial Dst for the IGY, *Ann. lnt. Geophys. Year*, 35, 9.

Sugiura, M. and Chapman S., 1960. The average morphology of geomagnetic storms with sudden commencements. *Abh. Akad. Wiss.* Gottingen, Sonderheft 4.

Takeuchi, A. Okubo, K. and Takeuchi, N., 2012. Electric Signals on and under the Ground Surface Induced by Seismic Waves, *International Journal of Geophysics.* Volume 2012, Article ID 270809, 10 pages, doi:10.1155/2012/270809.

Takla E., A. Khashaba, Abdel Zaher M., Yoshikawa A. and Uozumi T., 2018. Anomalous ultra-low frequency signals possibly linked with seismic activities in Sumatra, Indonesia. *NRIAG Journal of Astronomy and Geophysics*, 7:2, 247-252. doi: 10.1016/j.nrjag.2018.04.004.

Thomas, C., Livermore, R. and Pollitz, F., 2003, Motion of the Scotia Sea plates. *Geophys. J. Int.,* 155, 789–804.

Tsurutani, BT and Gonzalez, WD., 1997. The interplanetary causes of magnetic storms. A review, (In) B T Tsurutam, W D Gonzalez, Y Kamide and J K Aiballo (Eds.) Magnetic Storms. Geophys. Monograph, 98, *AGU*, Washington, D. C., 77-89.

Tsurutani, BT, Kamide, Y. Arballo, JK, Gonzalez, WD and Lepping, R. P., 1999. Interplanetary causes of great and super intense magnetic storms, P*hysics and Chemistry of the Earth*, 24, 101.

U.S. Geological Survey, 2019. Scientific Agency of the Department of the interior, https://earthquake.usgs.gov/earthquakes/ last accessed on June 5, 2019.

Varotsos P. A., Sarlis N.V., Skordas E.S., Lazaridou M.S., 2013, Seismic Electric Signals: An additional fact showing their physical interconnection with seismicity, Tectonophysics, Volume 589, 116-125, doi.org/10.1016/j.tecto.2012.12.020.